ISBN: 978-3-95450-168-7 doi:10.18429/JACoW-IPAC2015-WEPJE024

PROGRESS ON THE STUDY OF DIRECT LASER ELECTRON ACCELERATION IN DENSITY-MODULATED PLASMA WAVEGUIDES *

M.-W. Lin, B. W. Morgan, and I. Jovanovic†, Department of Mechanical and Nuclear Engineering, The Pennsylvania State University, University Park, PA 16802, U.S.A.
C.-Y. Hsieh, Y.-L. Liu, and S.-H. Chen, Department of Physics, National Central University, Jhongli 32001, Taiwan

Abstract

Direct laser acceleration of electrons can be achieved by utilizing the axial field of a guided, radially polarized laser pulse in a density-modulated plasma waveguide. When a short fs electron bunch is injected together with the drive laser pulse, our particle-in-cell simulations show that the electrostatic field, arising from plasma electrons perturbed by the laser ponderomotive force, increases the transverse divergence of the bunch electrons. Simulations are performed to study the method in which a precursor electron bunch is introduced prior to the main accelerated bunch. The precursor induces a focusing electrostatic field in the background plasma, which can considerably reduce the transverse expansion of the accelerated electrons. Based on the ignitor-heater scheme, density-modulated plasma waveguides are produced in experiments with high-Z gas targets and used to test the guiding of laser pulses. Supersonic gas jet nozzles for producing gas targets are simulated, designed, and then fabricated via additive manufacturing. Surface quality of the nozzles is evaluated via computed tomography.

INTRODUCTION

By guiding a radially polarized laser pulse in a density-modulated plasma waveguide, a large axial acceleration gradient on the order of tens of GV/m can be produced and used for direct laser acceleration (DLA) of electrons over an extended distance [1, 2]. The plasma waveguide extends the acceleration distance and the density modulation provides the quasi-phase matching (QPM) condition to improve the DLA efficiency. However, in addition to interacting with the laser fields, the injected bunch electrons also experience the nonlinear laser ponderomotive force and the electrostatic force from the resulting density variation of the background plasma electrons. The donut-shaped ponderomotive force of a radially polarized pulse pushes the plasma electrons to concentrate at the axis, which produces a transverse electrostatic force that can significantly defocus the electrons of a fs bunch after DLA [3].

In this study, we simulated the DLA scheme in which an additional precursor electron bunch is injected at a proper time prior to the main accelerated electron bunch. The precursor induces a focusing electrostatic field in the background plasma that can be used to considerably reduce the final transverse expansion of the accelerated electron bunch [4]. An all-optical method was experimentally implemented to produce density-modulated plasma channels with Ar gas target, which can be applied to realize the QPM of DLA. Next, micrometer-scale supersonic gas jet nozzles were designed and simulated for generating uniform gas density profiles needed for plasma waveguide production. Additive manufacturing techniques were applied to produce the nozzles.

DLA WITH A PRECURSOR

We carried out 3-D PIC simulations of DLA by the simulation framework VORPAL. Figure 1(a)-(c) summarizes the definition for the laser pulse for driving DLA and the 2.1-mm long plasma waveguide composed of alternating waveguide and neutral hydrogen sections that provide the necessary QPM condition. The waveguide sections have

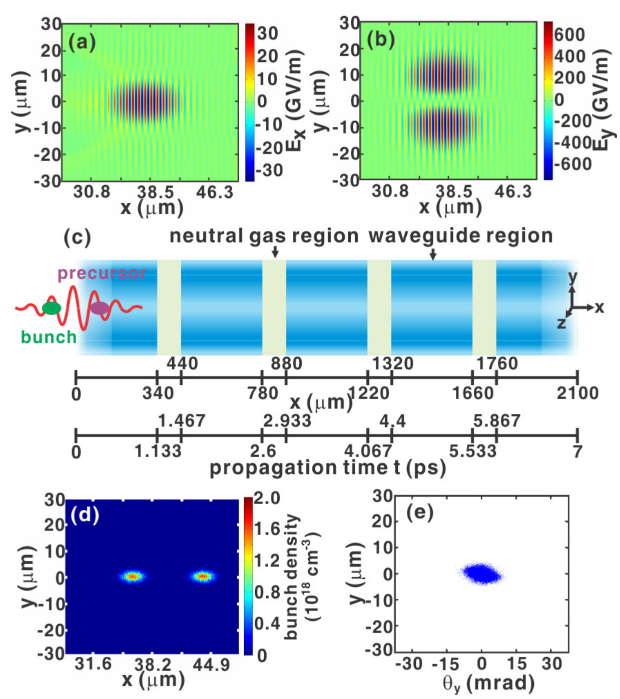

Figure 1: Snapshots of (a) longitudinal E_x and (b) transverse E_y electric fields of a 20-fs, 0.5-TW, radially polarized laser pulse pulse with a diameter of 15 μm; (b) illustration of a density-modulated plasma waveguide; (d) 2-D density distribution of the 6-fs, 40-MeV electron bunch and precursor injected in the simulation; (e) the trace space distribution for the bunch electrons shown in (d).

* Work supported by the United States Defense Threat Reduction Agency and the Ministry of Science and Technology in Taiwan.
† ijovanovic@psu.edu

ISBN: 978-3-95450-168-7 doi:10.18429/JACoW-IPAC2015-WEPJE024

a transverse plasma density profile in which density increases quadratically along the transverse axis from the central density of n_{e0}=2.5×10^{18} cm^{-3}. Neutral hydrogen gas sections have a uniform density distribution with density n_0=1.25×10^{19} cm^{-3} and are ionized by the laser pulse to produce uniform plasmas. Figure 1(d) shows a snapshot of the density profiles of the electron bunch and the precursor after injection. The 6-fs, 40-MeV electron bunch is defined with transverse and longitudinal Gaussian shape, a diameter w_b = 3 µm, and total charge of q_b = 5 pC. With identical parameters, the precursor is injected in advance of the accelerated bunch by a quarter of the plasma wavelength (∼ 5.3 µm). As shown in Fig. 1(e), the trace space distribution of the bunch electrons can be analyzed to understand the variation of the bunch transverse properties. The default RMS normalized emittance in y-dimension is calculated as $\epsilon_{N,y} \simeq 1\pi$ mm-mrad by the definition :

$$\epsilon_{N,y} = \frac{4}{m_e c}\sqrt{\langle y^2\rangle\langle P_y^2\rangle - \langle yP_y\rangle^2}\,\pi \ \text{mm} - \text{mrad}, \quad (1)$$

utilizing the particle positions y and momenta P_y.

When a single 6-fs long bunch is injected, Fig. 2(a) illustrates the on-axis bunch density $n_b(x)$, the variation of the on-axis plasma electron density $n_{pe}(x)$, and the on-axis total axial field $E_x(x)$ which accounts for the axial field of the laser pulse and the electrostatic field from the resulting density variation of the background plasma electrons. The bunch expels the plasma electrons and an ion channel, able to provide a focusing force to the bunch electrons, is gradually formed following the front edge of the bunch. However, the majority of bunch electrons do not experience a strong focusing force from the created ion channel since the variation of $n_{pe}(x)$ is of order ∼ 5.3 µm for its falling edge. As a result, the bunch electrons have an overall tendency to diverge throughout DLA, such as the final electron particle (within $|z|$ <0.4 µm) and trace space distributions shown in Fig. 2(c). The effect of the precursor and be observed in Fig. 2(b). The precursor depletes the plasma electrons in front of the bunch and creates a well-established ion channel that encloses all of the bunch electrons. Therefore, the final collimation of the bunch electrons can be significantly improved, as illustrated in Fig. 2(d), when compared to Fig. 2(c) for the results without a precursor. As shown in Fig. 2(f), the final bunch emittance $\epsilon_{N,y}$ is reduced from 14 π mm-mrad to 8.5 π mm-mrad when a precursor is introduced. The comparison of electron energy spectra plotted in Fig. 2(e) indicates an increased electron number in the range 55–70 MeV when a precursor is applied, which is attributed to the reduced bunch divergence (illustrated in Fig. 2(d)). As more electrons remain in the region where the laser field is intense, the fraction of electrons accelerated to higher energies is increased.

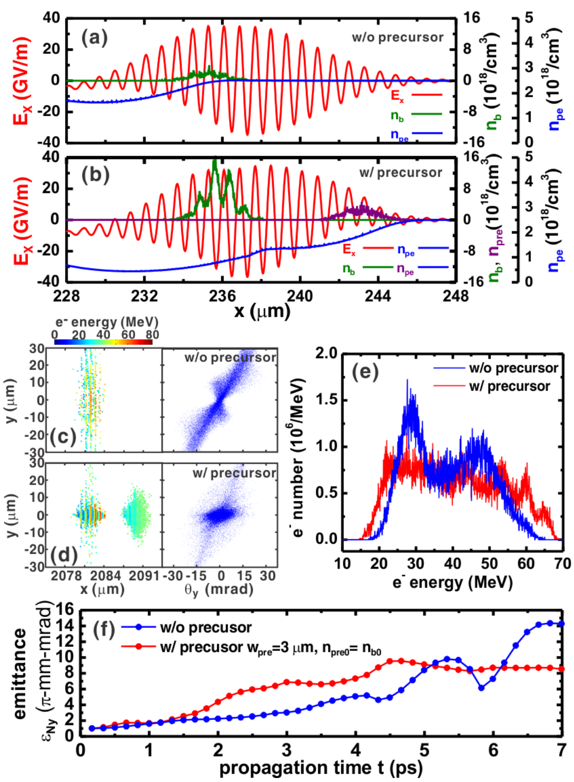

Figure 2: (a)-(b) Comparison of the sampled on-axis axial field E_x, on-axis plasma electron density n_{pe}, and densities of bunch n_b and precursor n_{pre}. (c)-(d) Final electron and trace space distributions, (e) final spectra, and (f) bunch emittance $\epsilon_{N,y}$ as a function of propagation time t for DLA with and without precursor.

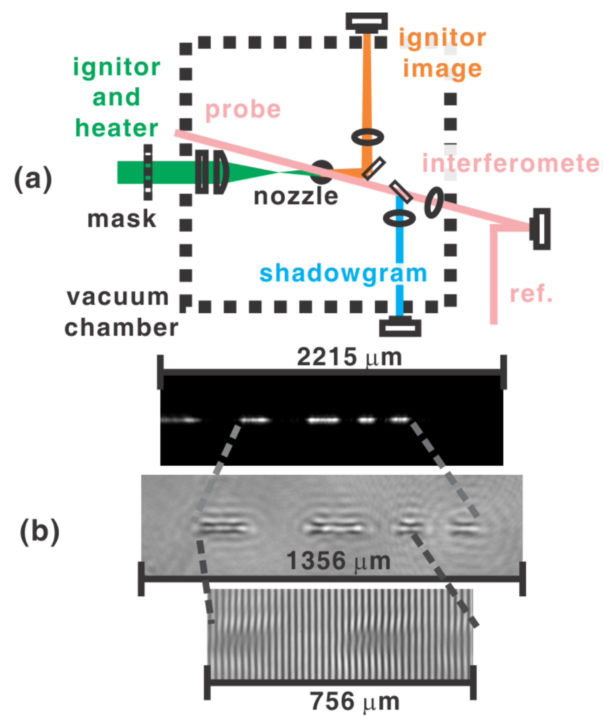

Figure 3: (a) Experimental layout of the plasma waveguide shaping system. (b) Intensity-modulated ignitor (upper) and the measured shadowgrams (center) and interferograms (lower) of the corresponding Ar plasma structure.

ISBN: 978-3-95450-168-7 doi:10.18429/JACoW-IPAC2015-WEPJE024

DENSITY-MODULATED PLASMA CHANNELS

Figure 3(a) shows the schematic diagram of the system developed to produce plasma waveguides. In the experiments, the Ar gas jet was produced by a 1.6-mm long slit nozzle, in which a 1.2-mm flat-top density profile can be obtained. The Ar backing pressure of 750 psi was selected to be fed into the gas valve for all experiments. By using the 90° geometry, the ignitor and heater beams are overlapped on top of the gas nozzle. The ignitor imaging system is used to monitor the on-target intensity pattern for laser pulse shaping. The shaped axial-structure of plasma waveguide can be diagnosed by the shadowgraphic image and the interferometer.

Using of 6.3-mJ ignitor, 36-mJ heater, and an ignitor-heater delay of 100 ps, Fig. 3(b) shows the intensity-modulated ignitor pattern, the corresponding transverse shadowgrams, and interferograms of the density-modulated Ar plasma structure. The ignitor pattern was created by passing the ignitor through a periodically cut mask and then imaging the ignitor with a demagnification of 5 on the target plane. The resulting shadowgrams and interferograms confirm the prediction that the plasma is produced in the regions where the ignitor and heater are spatially overlapped. This result provides the proof-of-principle foundation for producing the density-modulated plasma waveguides via the laser machining technique for future DLA experiments.

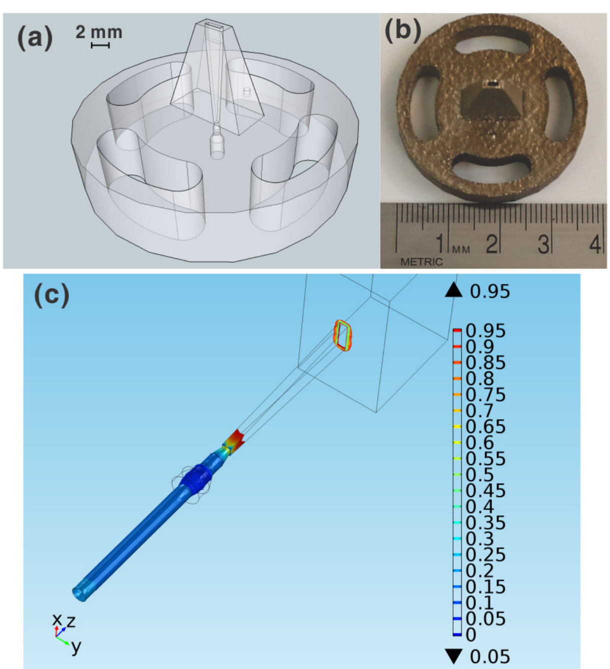

Figure 4: (a) Final supersonic micrometer slit jet design presented within the surrounding transparent support structure. (b) Final slit jet design manufactured in titanium through additive manufacturing. (c) Subsonic regions in the micrometer gas jet flow system produced in COMSOL to examine shockwave development. Shock waves only developed at the exterior edge of the nozzle exit where the gas velocity transitions to nonlinear flow.

SUPERSONIC GAS JET NOZZLES

Supersonic micrometer gas jet nozzles were designed based upon the de Laval valve using isentropic compressible fluid dynamics. The nozzle design was required to produce a gas number density profile of 1.25×10^{19} cm^{-3} at a height of 500 µm above the nozzle putlet, 2 mm in length parallel to the pump pulse propagation, and 500 µm in width perpendicular to the pump pulse propagation. The final nozzle design to produce the desired outlet density for helium and nitrogen is shown in Fig. 4(a). COMSOL Multiphysics high mach number flow simulation was used to test the isentropic compressible fluid dynamics design solution, to examine the effects of wall friction on the flow, and to identify shock wave development regions in the flow. Wall friction effects on the isentropic solution were substantial, requiring an increase in the design reservoir pressure from 100 psi to 180 psi to achieve the desired density profile. Shock waves were not found to develop in the flow system simulation due to a sufficient backing pressure to reservoir pressure ratio. Figure 4(c) is a COMSOL simulation of the de Laval valve depicted in Fig. 4(a) and shows the subsonic regions of flow velocity in the flow system from the pulse valve exit to the vacuum chamber.

Computed tomography was used to examine the surface feature size of the nozzles fabricated from titanium by additive manufacturing techniques at the Pennsylvania State University's Applied Research Laboratory. The internal surface features on the flow system wall had a maximum length of 300 µm in length and 140 µm in height perpendicular to the wall surface. The deformities can be reduced by use of electropolishing and abrasive techniques. The final nozzle produced from titanium by additive manufacturing is shown in Fig. 4(b).

CONCLUSION

PIC simulations were performed to study the improvement of the final bunch transverse properties in DLA when an additional precursor electron bunch is injected. By using the ignitor-heater scheme, Ar plasma channels could be fabricated with an appropriate axial density structure when a spatially modulated ignitor was introduced. Micrometer-scale supersonic de Laval slit jet nozzles were designed and produced by additive manufacturing techniques with dimensions that could not be readily obtained using traditional subtractive manufacturing techniques (machining).

REFERENCES

[1] P. Serafim, IEEE Trans. Plasma Sci. **28**, 1155 (2000).
[2] A.G. York *et al.*, Phys. Rev. Lett. **100**, 195001 (2008).
[3] M. -W. Lin *et al.*, Phys. Plasmas **21**, 093109 (2014).
[4] P. Chen, *et al.*, IEEE Trans. Plasma Sci. **PS-15**, 218 (1987).